Carrier-Induced Degradation in Multicrystalline Silicon: Dependence on the Silicon Nitride Passivation Layer and Hydrogen Released During Firing

Carlos Vargas, Kyung Kim, Gianluca Coletti, David Payne, Catherine Chan, Stuart Wenham, and Ziv Hameiri

***Abstract*—Carrier-induced degradation (CID) of multicrystalline silicon (mc-Si) solar cells has been receiving significant attention; however, despite this increasing interest, the defect (or defects) responsible for this degradation has not been determined yet. Previous studies have shown that the surface passivation layer and the firing temperature have a significant impact on the rate and extent of this degradation. In this paper, we further study this impact through an investigation of the CID behavior of the mc-Si wafers passivated with six different silicon nitride layers, each fired at four different peak temperatures. At low firing temperatures, no significant difference in the CID was identified between the samples with different passivation layers; however, a large range of degradation extents was observed at higher firing temperatures. Using Fourier transform infrared spectroscopy, a correlation was found between the degradation extent and the amount of hydrogen released from the dielectric during firing. We verified that no degradation of the surface passivation quality occurred, indicating that the degradation is primarily associated with a bulk defect.**

***Index Terms*—Degradation, multicrystalline silicon (mc-Si), solar cells, silicon nitride.**

I. Introduction

RAMSPECK *et al*. [1] were the first to report the degradation of *p*-type multicrystalline silicon (mc-Si) solar cells when exposed to light and elevated temperatures; this effect was later named LeTID (light and elevated temperature-induced degradation) [2]. Subsequently, Kersten *et al*. [2] reported that the degradation also occurs when using current injection and is faster under an open-circuit condition than under a short-circuit condition. Therefore, the degradation is also known as carrier-induced degradation (CID) [2], [3]. Efficiency losses of up to 16% (relative) on the passivated emitter rear cells (PERC) fabricated on the mc-Si substrates have been reported [4]. Since it is expected that the mc-Si PERC will become the dominant technology in the photovoltaic industry for the next years [5], this degradation is currently receiving significant attention [2]–[4], [6]–[16].

The nature of the defect responsible for the CID in *p*-type mc-Si is still unknown. As Ramspeck *et al*. reported the CID on gallium (Ga) doped mc-Si [1], and since the interstitial oxygen concentration is lower in the mc-Si than in Czochralski (Cz) silicon [17], the formation of a boron-oxygen (B-O) complex has been discarded as the primary cause. In addition, the time scales of CID formation and regeneration are much slower than those of the B-O and iron-boron pairs [1]–[3]. Inglese *et al.* [18] suggested a possible involvement of copper (Cu) in the CID after the detection of an enhanced degradation rate in the Cu-contaminated mc-Si wafers (both B and Ga doped). However, Cu involvement has not been supported yet by lifetime spectroscopy measurements. Such measurements have been recently reported by Morishige *et al.* [12] and Vargas [13]. The Shockley–Read–Hall recombination parameters of the CID-associated defect have been extracted and are similar to that of titanium (Ti) and molybdenum (Mo), which are therefore possible candidates [12], [13]. Tungsten (W) was also suggested by Morishige *et al.* [12]; however, its recombination parameters are quite different from those determined later by temperature- and injection-dependent lifetime spectroscopy measurements [13]. However, due to the uncertainty in the literature regarding defect values and the possibility of a defect that has not been yet identified, it has not yet been possible to determine with certainty the specific defect responsible for CID.

The surface passivation layer appears to play an important role in the CID [6], [7], [19], [20]. Fertig *et al.* reported a more pronounced degradation in the mc-Si cells with an aluminum oxide (AlO_x) passivation layer than in the aluminum back sur-

Manuscript received August 7, 2017; revised October 2, 2017 and November 21, 2017; accepted December 4, 2017. Date of publication January 11, 2018; date of current version February 16, 2018. This work was supported by the Australian Government through the Australian Renewable Energy Agency under Project 2014/RND097. The work of Z. Hameiri was supported by the Australian Research Council through the Discovery Early Career Researcher Award under Project DE150100268. *(Corresponding author: Carlos Vargas.)*

C. Vargas, K. Kim, D. Payne, C. Chan, and Z. Hameiri are with the School of Photovoltaic and Renewable Energy Engineering, University of New South Wales, Sydney, NSW 2052, Australia (e-mail: c.vargascastrillon@student.unsw.edu.au; k.h.kim@student.unsw.edu.au; d.n.payne@unsw.edu.au; catherine.chan@unsw.edu.au; ziv.hameiri@gmail.com).

G. Coletti is with the School of Photovoltaic and Renewable Energy Engineering, University of New South Wales, Sydney, NSW 2052, Australia, and also with the Energy Research Centre of the Netherlands, Petten 1755, The Netherlands (e-mail: coletti@ecn.nl).

S. Wenham, deceased, was with the School of Photovoltaic and Renewable Energy Engineering, University of New South Wales, Sydney, NSW 2052, Australia.

Color versions of one or more of the figures in this paper are available online at http://ieeexplore.ieee.org.

Digital Object Identifier 10.1109/JPHOTOV.2017.2783851

TABLE I
DEPOSITION CONDITIONS AND LAYER PROPERTIES BEFORE FIRING

Passivation layer label	Deposition temp. (°C)	Gas ratio (NH_3/SiH_4)	Pressure (mbar)	Thickness (nm)	RI (at 633 nm)	Hydrogen concentration
SiN_x–1	442	2.25	0.17	121.9	2.13	9.92%
SiN_x–2	442	4.00	0.33	107.7	2.14	10.34%
SiN_x–3	400	2.25	0.17	120.5	2.14	11.13%
SiN_x–4	400	4.00	0.33	109.6	2.14	11.36%
SiN_x–5	350	2.25	0.17	121.8	2.12	12.15%
SiN_x–6	350	4.00	0.33	113.0	2.12	12.41%

face field (Al-BSF) cells [7]. Therefore, they concluded that the AlO_x surface passivation likely played a role in the CID. Differences in degradation rates and extents between PERC and Al-BSF cells were also reported by Padmanabhan *et al.* [20]. Recently, Kersten *et al.* reported different CID rates for mc-Si lifetime samples passivated with AlO_x, silicon nitride (SiN_x) and AlO_x/SiN_x stack layers [6]. Specifically, they used SiN_x layers deposited by two different industrial systems and reported differences in the resulting degradation rates. This was the first indication that the SiN_x properties can influence the CID reaction rates. However, the exact deposition conditions and SiN_x properties were not reported [6]. In addition, Kersten *et al.* [19] reported different degradation extents when using different AlO_x passivation layers deposited by atomic layer deposition. More recently, Sperber *et al.* [21] reported surface passivation quality changes over time because of light and elevated temperature of SiN_x and AlO_x layers deposited on float zone wafers; however, to date, these changes in the surface passivation quality have not been correlated with CID. Furthermore, a study conducted by Nakayashiki *et al.* [10] clearly demonstrated a degradation of the bulk minority carrier lifetime after light soaking, indicating that the CID has a strong bulk component. This conclusion was also supported by Padmanabhan *et al.* [20], as complete regeneration was found in both Al-BFS and PERC structures.

It has also been reported that the CID has a strong dependence on the firing temperature used to form the metal contacts of screen printed solar cells [8], [10], [14], [16]. Higher peak firing temperatures lead to a more pronounced degradation. CID is less severe in samples fired at low temperature (< 600 °C), and it is not present in nonfired samples [8]. This particular fact is consistent with the hypothesis suggested by Bredemeier *et al.* [16], who suggest the dissolution of precipitate impurities. On the other hand, Zuschlag *et al.* [15] have demonstrated that different phosphorus diffusions and gettering lead to different the CID behavior. In general, it appears that the thermal history of the wafers has an influence on the CID temporal dependence and extent [9]. Furthermore, if the influence of the hydrogenated surface passivation layer and the firing step are considered together, hydrogen appears to be a candidate involved in the formation of the CID as has been suggested by Chan *et al*. [9] and Jensen *et al.* [11].

In this contribution, evidence of the impact of the properties of the SiN_x passivation layer on the CID is presented for four different peak firing temperatures. A correlation is found between the hydrogen fraction released during the firing and the CID extent, suggesting a possible involvement of hydrogen in the degradation. The unchanged surface saturation current during the degradation indicates that the observed CID is likely caused by a bulk defect.

II. MATERIAL AND METHODS

This experiment was conducted using two sets of six neighboring six-inch conventional *p*-type mc-Si wafers from central bricks with a thickness of 0.019 cm and resistivity of 1.6 Ω.cm (Set I) and 1.9 Ω.cm (Set II), and one set of six double-side polished Cz wafers used for Fourier transform infrared spectroscopy (FTIR) measurements (thickness 0.02 cm and resistivity 1.0 Ω·cm). Symmetrical lifetime test structures were formed using the mc-Si wafers, representing the front surface of a PERC solar cell (phosphorous-diffused surface passivated with SiN_x): The wafers were initially cleaned using the Radio Corporation of America (RCA) process, followed by a light phosphorous diffusion (both sides; carried out in a Tempress $POCl_3$ tube) to form an *n*-doped layer with a sheet resistance of 80 Ω/□. Subsequently, the wafers received a hydrofluoric acid (HF) dip to remove the phosphosilicate glass. These test structures were divided into six different groups (one wafer from each set). Each group was then symmetrically deposited with a different SiN_x layer (front and rear) using a Meyer Burger MAiA plasma-enhanced chemical vapor deposition system (see Table I for the deposition conditions and properties of each layer). In parallel, the Cz wafers were RCA cleaned and then received SiN_x deposition on the front side (one wafer per layer; without phosphorus diffusion). The used SiN_x films are based on our recent work [22] targeting a similar refractive index (RI) and good surface passivation quality, yet with different hydrogen content between samples.

The six-inch mc-Si wafers were laser cleaved into 3.9 cm × 3.9 cm tokens. Four tokens from each wafer underwent firing at four different peak temperatures, forming four sets of six sister tokens [(653 ± 9) °C, (748 ± 3) °C, (795 ± 9) °C, and (825 ± 7) °C; actual temperature as measured by a Datapaq Q18 furnace temperature profiler using tokens from the same wafers].

The six Cz (FTIR) wafers were fired at one temperature [(748 ± 7)°C]. After the FTIR measurements, the films were removed using an HF dip to return the wafers to their original state. Comparing FTIR measurements of wafers after this process to

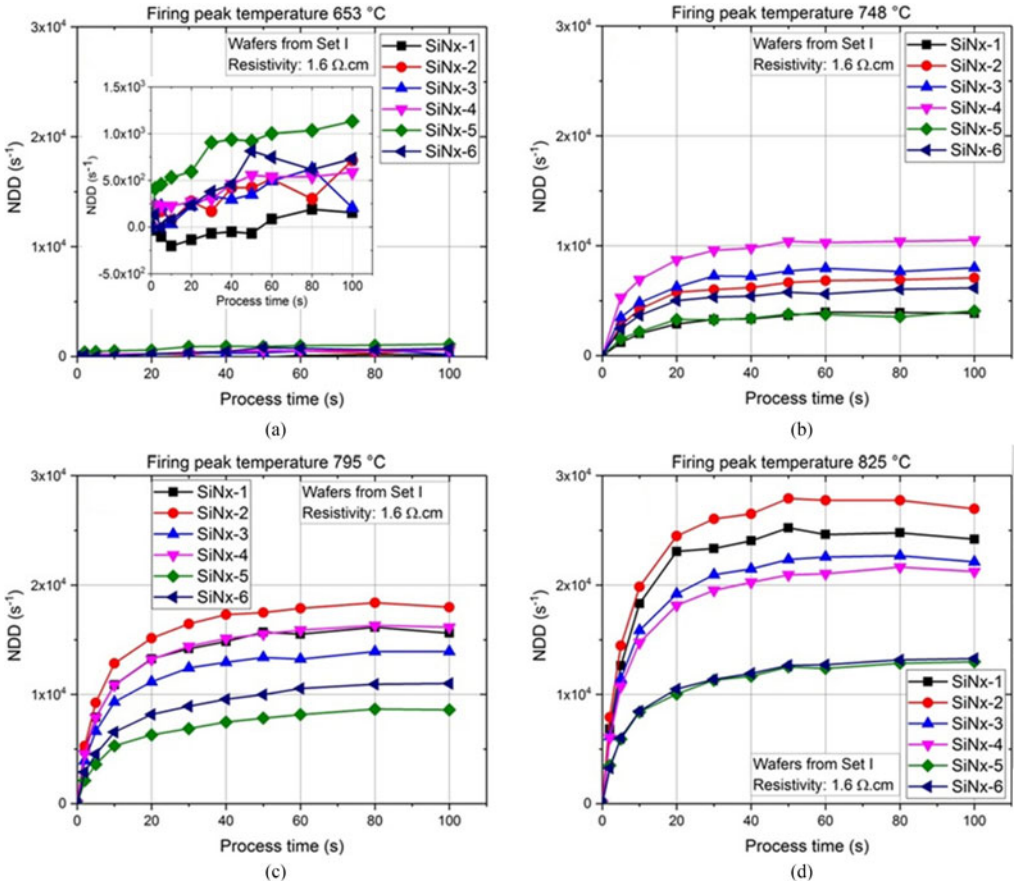

Fig. 1. NDD as a function of cumulative laser process time for different SiN_x layers fired at (a) 653 °C, (b) 748 °C, (c) 795 °C, and (d) 825 °C. The inset in (a) corresponds to the same data plotted using a different scale (the lines are a visual aid for the reader).

those of an unprocessed bare wafer confirmed that the wafers returned to their initial state, as no difference was observed between the spectra. The wafers were then RCA cleaned, before SiN_x depositions of the same layers. The wafers were then fired at the next temperature; this sequence was repeated twice in order to investigate three peak firing temperatures [(748 ± 7) °C, (799 ± 9) °C, and (827 ± 2) °C].

In accordance with the laser-accelerated degradation and regeneration process proposed by Payne *et al.* [3], the mc-Si wafers were degraded using a 938-nm laser at an intensity of 46 kW/ m^2 and wafer temperature of 140 °C. This process was applied for different time steps, starting with the shortest interval (2 s) in progressive steps until maximum degradation was reached (100 s), allowing for clear identification of any differences in the CID extent for each wafer.

After each laser process, the changes in the effective lifetime of the sample were monitored using a photoconductance lifetime tester (WCT-120, Sinton instruments at a sample temperature of 30 °C) along with photoluminescence (PL) imaging (BTI LIS-R1). The lifetime measurements were done at quasi-steady-state conditions and were analyzed using the generalized method [23]. The Cz polished wafers were used to characterize the optical properties of the layer (thickness and RI) using ellipsometry. The FTIR transmission spectra were measured using an FTIR spectrometer (Nicolet 5700 from Thermo). Three distinguished absorption peaks were identified, which were associated with Si–N (880 cm^{-1}), Si–H (2220 cm^{-1}), and N–H (3340 cm^{-1}) vibrational modes. The bond concentration [*A*–*B*] was calculated using [22], [24]

$$[A-B] = k_{A-B} \int \frac{\alpha(\omega)}{\omega} d\omega \tag{1}$$

where $\alpha(\omega)$ is the absorption coefficient at wavenumber ω, and k_{A-B} is the proportionality constant as taken from [25]. In this study, hydrogen fraction is defined as ([Si–H] + [N–H])/([Si–H] + [N–H] + [Si–N]). The hydrogen fraction of the films after the deposition is presented at Table I. We estimate the repeatability of the calculated hydrogen fraction as 1.5% (standard deviation), based on measurements carried out on the same wafer at different points and days. This value is significantly smaller than the measured differences in the hydrogen fractions of the layers used in this experiment (see Table I).

III. Results and Discussion

Due to a small difference in the surface passivation quality of the six SiN_x layers and the inhomogeneous nature of mc-Si wafers, a standard deviation of 14% in the effective lifetimes of tokens fired at the same condition was found (after firing); it corresponds to a deviation of 9 μs from a mean value of 62 μs

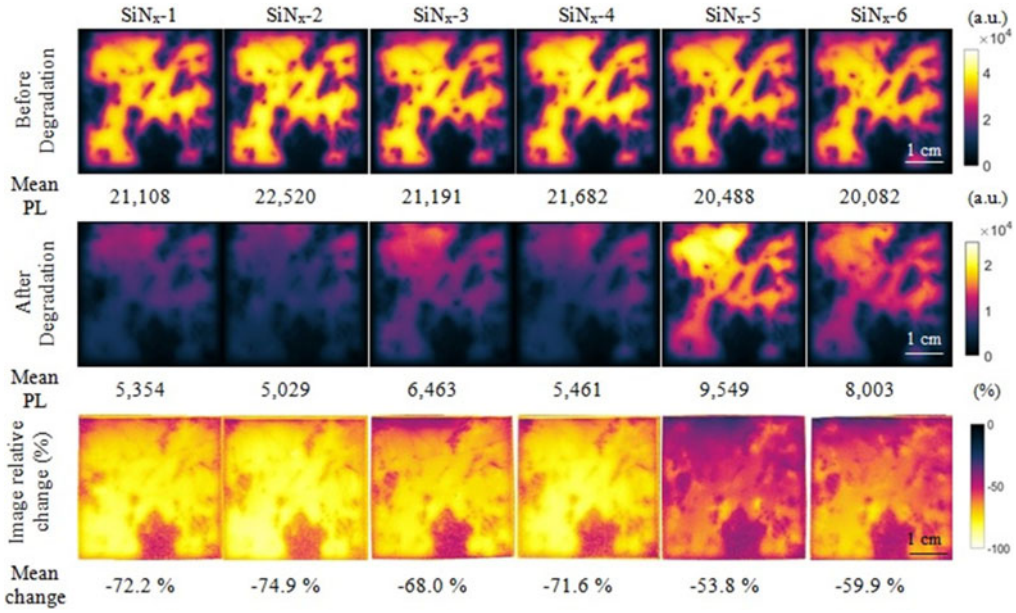

Fig. 2. Uncalibrated PL images before and after laser degradation of Set I tokens fired at 795 °C. The numbers below each image are the mean PL counts (please note that two different color scales were used before and after the degradation to enhance the image contrast). The image ratio between the undegraded and degraded state is also presented.

(tokens from Set I fired at 825 °C). Accordingly, the normalized defect density (NDD) was used for the analysis; it is defined as

$$\mathrm{NDD}\,(t) = \frac{1}{\tau\,(t)} - \frac{1}{\tau_{\mathrm{fire}}} \tag{2}$$

where τ_{fire} and $\tau(t)$ are the effective lifetimes after firing and after laser degradation process time t, respectively. They were taken at an excess carrier concentration (Δn) of 10^{15} cm^{-3}.

Fig. 1(a)–(d) presents the NDD of the tokens from Set I to be a function of the cumulative laser process time. Similar results were obtained for the wafers from Set II. Based on tests carried out on similar wafers, we estimate the repeatability associated with the effective lifetime measurements to be in the range of 2%.

At low firing temperature [see Fig. 1(a)], the observed degradation was weak to negligible, as also reported by others [8]. No significant differences in the NDD behavior were found among the different SiN_x layers. Higher firing temperatures made the CID more pronounced [see Fig. 1(b)–(d)] and significant differences in degradation characteristics between the different SiN_x layers can be observed in these cases. Differences are most evident at the firing temperature of 795 °C, a temperature that is the most relevant for contacts formation after silver screen printing, as most of the pastes require peak firing temperatures of around 800 °C [26]. Fig. 2 provides the PL images of the set of samples fired at 795 °C (Set I) after firing and in the most degraded state, together with images of the calculated relative change defined as $(I_{\mathrm{aft}} - I_{\mathrm{bef}})/I_{\mathrm{bef}} \times 100\%$, where I_{bef} and I_{aft} are the PL images before and after the degradation. All the PL images were taken with an exposure time of 0.3 s using a 810-nm laser with a photon flux of 2.55×10^{17} cm^{-2}s^{-1}; the images were processed using the recently developed software described elsewhere [27]. It is easy to observe the difference in degradation between the

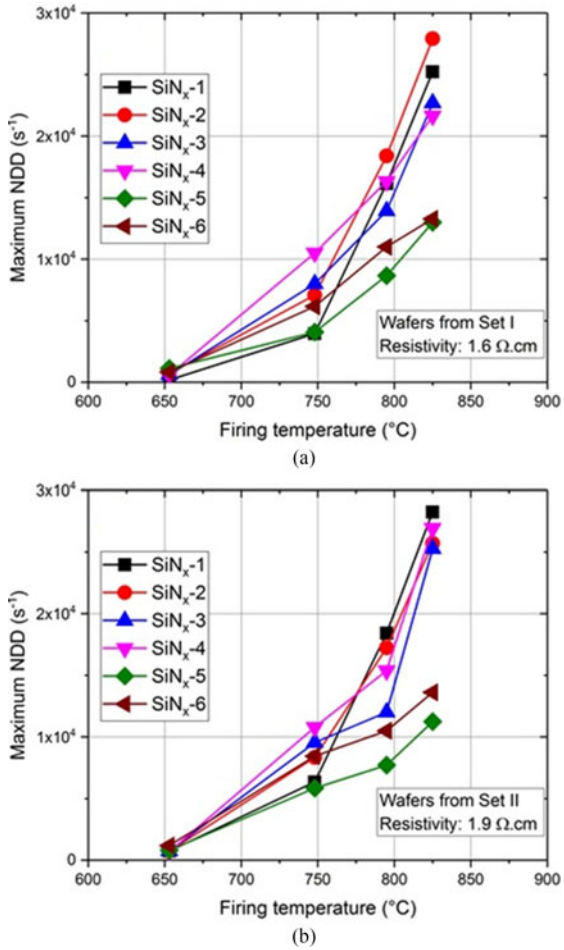

Fig. 3. Maximum NDD for different firing temperatures and SiN_x passivation layers for the two sets of wafers (the lines are a visual aid for the reader).

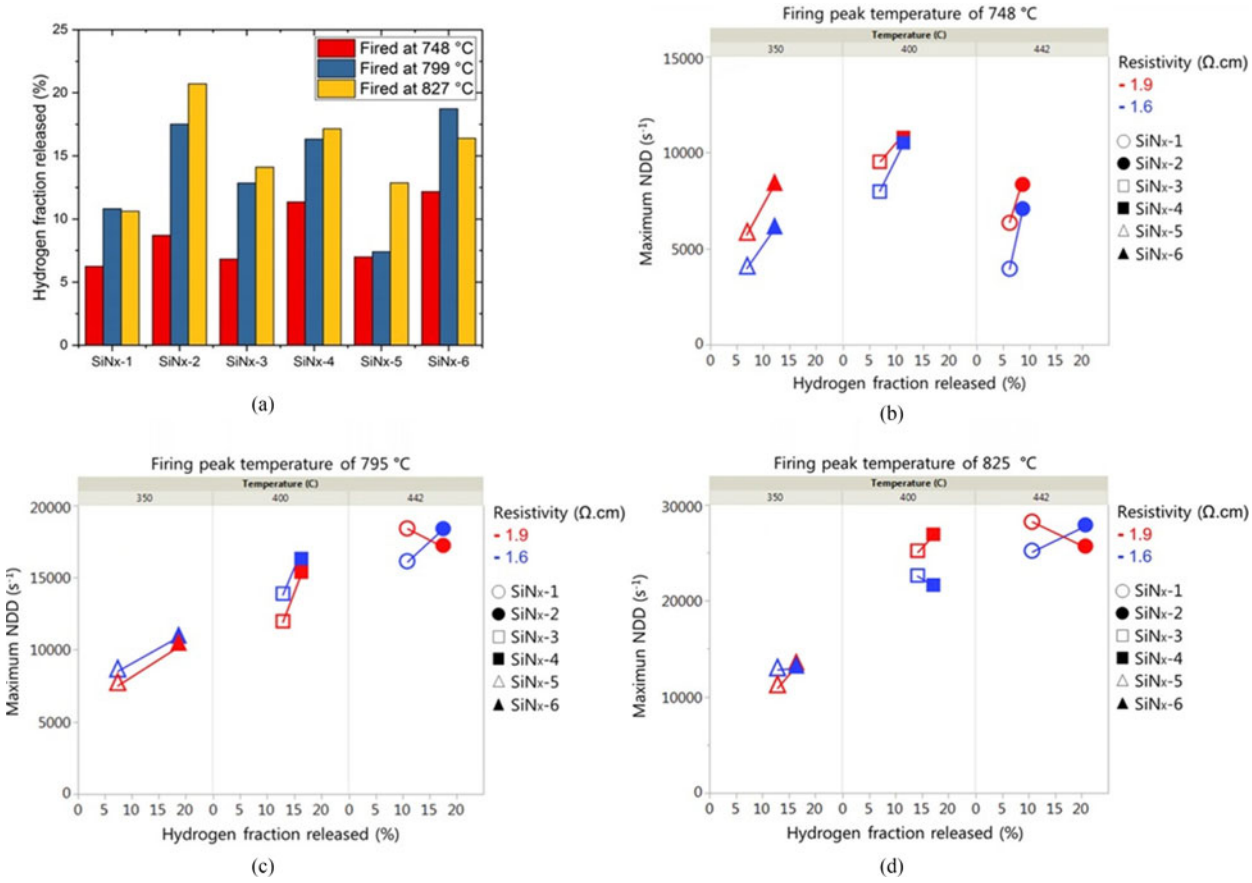

Fig. 4. Comparison between the hydrogen fraction released during the firing and the CID extent: (a) Hydrogen fraction released as a function of the peak firing temperature. Maximum NDD versus the hydrogen released fraction for (b) 748 °C, (c) 795 °C, and (d) 825 °C. The lines are given as a guide to the eyes illustrating the trend.

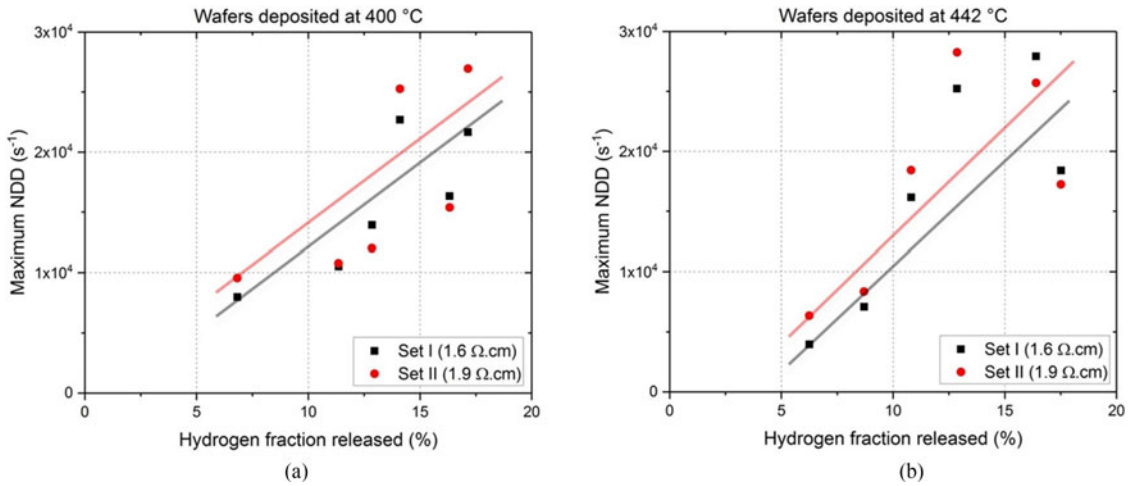

Fig. 5. Maximum NDD as a function of the hydrogen fraction released for fixed deposition temperatures: (a) 400 °C and (b) 442 °C. The lines are given as a guide to the eyes illustrating the trend.

SiN_x recipes used in this experiment, as expected from Fig. 1(c). It appears that dislocated areas degraded less compared with regions with lower dislocation density; however, the degradation is quite uniform through the large grain areas. Fig. 3 presents the maximum NDD for the two sets of wafers (Sets I and II). Both sets present a similar firing dependence despite the slight difference between the degradation extents. In addition, the absolute value of the mean relative change of the PL counts (see Fig. 2) follows a similar trend, as is illustrated in Fig. 3.

Thus far, the results indicate that different SiN_x layers lead to different CID extents and that the difference is more evident when high peak firing temperatures are used. These results are

consistent with the work from Kersten *et al.* [6] in which samples with SiN_x layers deposited using two different industrial systems, and most probably with different properties, showed differences in the degradation time dependence and extent. Particularly, our work shows that SiN_x layers deposited at low temperature show less degradation.

As discussed above, previous studies have suggested a possible involvement of hydrogen in the CID [9], [11]. Consequently, we now test for a correlation of the degradation extent with the hydrogen fraction released from the film during the firing process. Although we are aware of the fact that not all the released hydrogen penetrates into the bulk [28], we assume that a higher amount of released hydrogen indicates that a higher amount of hydrogen penetrates into the wafer. We are also aware of the possible impact of the diffused *n*-type layer on the penetration of hydrogen into the mc-Si wafers (in comparison to the undiffused FTIR wafers); however, we assume that the effect related to this layer is the same for all of the mc-Si wafers studied, as they were all diffused together. Based on FTIR measurements, Fig. 4 presents this correlation. The hydrogen fraction released during the firing is calculated as $[\mathrm{H}]_{\mathrm{rel}} = ([\mathrm{H}]_{\mathrm{dep}} - [\mathrm{H}]_{\mathrm{fired}})/[\mathrm{H}]_{\mathrm{dep}} \times 100\%$, where $[\mathrm{H}]_{\mathrm{dep}}$ and $[\mathrm{H}]_{\mathrm{fired}}$ are the hydrogen fractions of the SiN_x layer as deposited and after the firing, respectively. According to our measurements, high initial hydrogen content (see Table I) does not necessarily mean higher hydrogen released [see Fig. 4(a)]; however, the cause of this lack of correlation is beyond the scope of this paper.

As can be seen in Fig. 4(a), higher firing temperatures led to a higher fraction of released hydrogen (with exception of SiN_x–6), this could possibly explain the stronger CID extent observed at higher firing temperatures [13]. In addition, as can be observed in Fig. 4(b)–(d), in the majority of cases, the degradation was more pronounced for wafers with SiN_x layers that released a higher amount of hydrogen during the firing process (15 out of the 18 tested cases). For instance, Fig. 5 presents the maximum NDD as a function of the hydrogen fraction released during the firing for deposition temperatures 400 °C [see Fig. 5(a)] and 442 °C [see Fig. 5(b)]. Again, it seems that there is a positive correlation between the released hydrogen and the extent of degradation. The nonperfect correlation can potentially be explained by other unintentional changes, such as those introduced by the firing of the wafers, differences between the pieces used for the different firing conditions, and measurement uncertainties. Note that only a weak correlation was observed when plotting the maximum NDD as a function of released hydrogen for all the films. This indicates a secondary dependence on the deposition temperature. Indeed, the layers deposited at lower temperature show minimum CID extent. This dependence can be explained by two factors: First, different deposition temperatures lead to change in layer densities as previously reported (for example in [22]); secondly, the CID appears to have a dependence on the thermal history of the sample, as discussed by Chan *et al.* [9].

In order to compare possible changes in the surface passivation quality because of the CID, the surface recombination saturation current (J_{os}) and the bulk lifetime at high injection

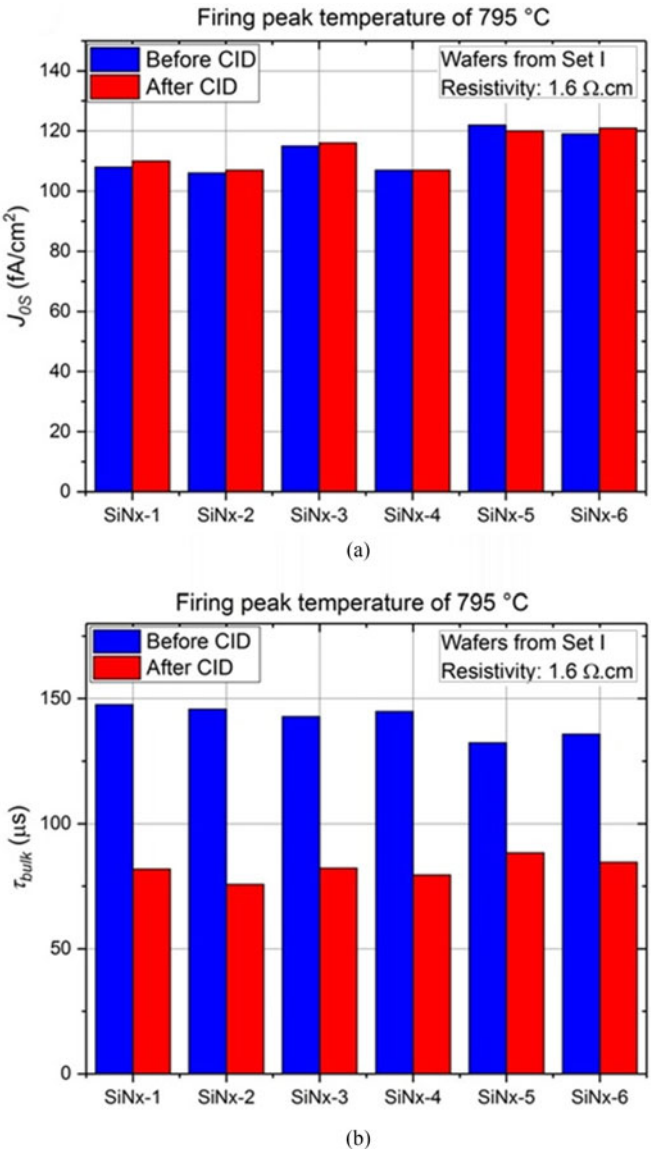

Fig. 6. Comparison between the changes in the surface saturation current density (a) and the bulk lifetime (b) before and after the degradation of wafers fired at 795 °C.

(τ_{bulk}) were extracted using the Kane and Swanson method [29] as implemented in the Sinton Instruments lifetime tester, before and after degradation (at $\Delta n = 2 \times 10^{16}\,\mathrm{cm}^{-3}$). No significant degradation of the surface passivation quality was observed (on the contrary, in some cases an improvement was detected), while τ_{bulk} changed considerably (see Fig. 6). Similar results were found for the wafers fired at other temperatures. Therefore, it can be concluded that the observed CID did not originate from a defect related to the surface.

IV. Conclusion

In this study, differences in the degradation extent were found between six different SiN_x layers, when high firing peak temperatures were used, indicating a dependence of the CID on the SiN_x passivation layer properties. According to our results, the wafers passivated with SiN_x layers deposited at lower temper-

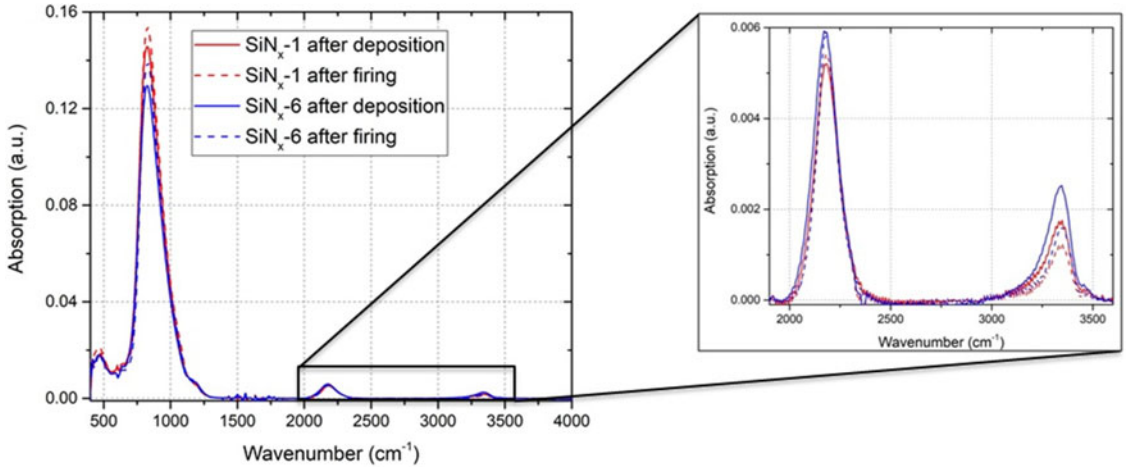

Fig. 7. Representative FTIR measurements of SiN_x–1 and SiN_x–6 before and after firing at 795 °C. Considering the change on the SiN and NH peaks, SiN_x–6 released more hydrogen than SiN_x–1.

atures presented less severe CID. FTIR measurements indicate a correlation between the hydrogen fractions released during the firing and the extent of the degradation. To the best of our knowledge, this is the first time that such a correlation has been reported. This provides evidence to suggest that hydrogen is involved, at least to some extent, in activating the recombination associated with the CID in mc-Si. Furthermore, no significant changes in the surface passivation quality were detected, and we therefore conclude that the observed CID is primarily associated with a bulk defect.

APPENDIX

Fourier Transform Infrared Spectroscopy Measurements: See Fig. 7.

ACKNOWLEDGMENT

The views expressed herein are not necessarily the views of the Australian Government, and the Australian Government does not either accept responsibility for any information or advice contained herein.

REFERENCES

[1] K. Ramspeck *et al.*, "Light induced degradation of rear passivated mc-Si solar cells," in *Proc. 27th Eur. Photovolt. Sol. Energy Conf. Exhib.*, vol. 27, 2012, pp. 861–865.

[2] F. Kersten *et al.*, "Degradation of multicrystalline silicon solar cells and modules after illumination at elevated temperature," *Sol. Energy Mater. Sol. Cells*, vol. 142, pp. 83–86, Nov. 2015.

[3] D. N. R. Payne *et al.*, "Acceleration and mitigation of carrier-induced degradation in *p*-type multi-crystalline silicon," *Phys. Status Solidi—Rapid Res. Lett.*, vol. 10, no. 3, pp. 237–241, Mar. 2016.

[4] Kai Petter *et al.*, "Dependence of LeTID on brick height for different wafer suppliers with several resistivities and dopants," in *Proc. 9th Int. Workshop Cryst. Silicon Sol. Cells*, 2016.

[5] M. A. Green, "The passivated emitter and rear cell (PERC): From conception to mass production," *Sol. Energy Mater. Sol. Cells*, vol. 143, pp. 190–197, Dec. 2015.

[6] F. Kersten, J. Heitmann, and J. W. Müller, "Influence of Al_2O_3 and SiN_x passivation layers LeTID," *Energy Procedia*, vol. 92, pp. 828–832, Aug. 2016.

[7] F. Fertig, K. Krauß, and S. Rein, "Light-induced degradation of PECVD aluminium oxide passivated silicon solar cells," *Phys. Status Solidi—Rapid Res. Lett.*, vol. 9, no. 1, pp. 41–46, Jan. 2015.

[8] C. E. Chan *et al.*, "Rapid stabilization of high-performance multicrystalline *p*-type silicon PERC cells," *IEEE J. Photovolt.*, vol. 6, no. 6, pp. 1473–1479, Nov. 2016.

[9] C. Chan *et al.*, "Modulation of carrier-induced defect kinetics in multicrystalline silicon PERC cells through dark annealing," *Phys. Status Solidi—Rapid Res. Lett.*, vol. 1, no. 2, Feb. 2017, Art. no. 1600028.

[10] K. Nakayashiki *et al.*, "Engineering solutions and root-cause analysis for light-induced degradation in *p*-type multicrystalline silicon PERC modules," *IEEE J. Photovolt.*, vol. 6, no. 4, pp. 860–868, Jul. 2016.

[11] M. A. Jensen, A. E. Morishige, J. Hofstetter, D. B. Needleman, and T. Buonassisi, "Evolution of LeTID defects in *p*-type multicrystalline silicon during degradation and regeneration," *IEEE J. Photovolt.*, vol. 7, no. 4, pp. 980–987, Jul. 2017.

[12] A. E. Morishige *et al.*, "Lifetime spectroscopy investigation of light-induced degradation in *p*-type multicrystalline silicon PERC," *IEEE J. Photovolt.*, vol. 6, no. 6, pp. 1466–1472, Nov. 2016.

[13] C. Vargas *et al.*, "Recombination parameters of lifetime-limiting carrier-induced defects in multicrystalline silicon for solar cells," *Appl. Phys. Lett.*, vol. 110, no. 9, Feb. 2017, Art. no. 092106.

[14] R. Eberle, W. Kwapil, F. Schindler, M. C. Schubert, and S. W. Glunz, "Impact of the firing temperature profile on light induced degradation of multicrystalline silicon," *Phys. Status Solidi—Rapid Res. Lett.*, vol. 10, no. 12, pp. 861–865, Dec. 2016.

[15] A. Zuschlag, D. Skorka, and G. Hahn, "Degradation and regeneration in mc-Si after different gettering steps," *Prog. Photovolt. Res. Appl.*, vol. 25, no. 7, pp. 545–552, Jul. 2017.

[16] D. Bredemeier, D. Walter, S. Herlufsen, and J. Schmidt, "Lifetime degradation and regeneration in multicrystalline silicon under illumination at elevated temperature," *AIP Adv.*, vol. 6, no. 3, Mar. 2016, Art. no. 035119.

[17] G. Coletti, C. L. Mulder, G. Galbiati, and L. J. Geerligs, "Reduced effect of B-O degradation on multicrystalline silicon wafers," in *Proc. 21st Eur. Photovol. Solar Energy Conf. Exhib.*, vol. 21, 2006, pp. 1515–1518.

[18] A. Inglese *et al.*, "Light-induced degradation in multicrystalline silicon: The role of copper," *Energy Procedia*, vol. 92, pp. 808–814, Aug. 2016.

[19] F. Kersten, I. Förster, and S. Peters, "Evaluation of spatial ALD of Al_2O_3 for rear surface passivation of mc-Si PERC solar cells," in *Proc. 32nd Eur. Photovolt. Sol. Energy Conf. Exhib.*, vol. 32, Jul. 2016, pp. 943–945.

[20] M. Padmanabhan *et al.*, "Light-induced degradation and regeneration of multicrystalline silicon Al-BSF and PERC solar cells," *Phys. Status Solidi—Rapid Res. Lett.*, vol. 10, no. 12, pp. 874–881, Dec. 2016.

[21] D. Sperber, A. Herguth, and G. Hahn, "Instability of dielectric surface passivation quality at elevated temperature and illumination," *Energy Procedia*, vol. 92, pp. 211–217, Aug. 2016.

[22] Z. Hameiri *et al.*, "Low-absorbing and thermally stable industrial silicon nitride films with very low surface recombination," *IEEE J. Photovolt.*, vol. 7, no. 4, pp. 996–1003, Jul. 2017.

[23] H. Nagel, C. Berge, and A. G. Aberle, "Generalized analysis of quasi-steady-state and quasi-transient measurements of carrier lifetimes in semiconductors," *J. Appl. Phys.*, vol. 86, no. 11, pp. 6218–6221, Dec. 1999.

[24] M. Cardona, "Vibrational spectra of hydrogen in silicon and germanium," *Phys. Status Solidi B*, vol. 118, no. 2, pp. 463–481, Aug. 1983.

[25] F. Giorgis *et al.*, "Optical, structural and electrical properties of device-quality hydrogenated amorphous silicon-nitrogen films deposited by plasma-enhanced chemical vapour deposition," *Philosph. Mag. Part B*, vol. 77, no. 4, pp. 925–944, Apr. 1998.

[26] Dupont.com, 'SOLAMET PV19A,' 2017. [Online]. Available: http://www.dupont.com/content/dam/dupont/products-and-services/solar-photovoltaic-materials/solar-photovoltaic-materials-landing/documents/Solamet-PV19A-Data-Sheet.pdf. Accessed on: Aug. 5, 2017.

[27] D. N. R. Payne, C. Vargas, Z. Hameiri, S. R. Wenham, and D. M. Bagnall, "An advanced software suite for the processing and analysis of silicon luminescence images," *Comput. Phys. Commun.*, vol. 215, pp. 223–234, Jun. 2017.

[28] S. Wilking, S. Ebert, A. Herguth, and G. Hahn, "Influence of hydrogen effusion from hydrogenated silicon nitride layers on the regeneration of boron-oxygen related defects in crystalline silicon," *J. Appl. Phys.*, vol. 114, no. 19, 2013, Art. no. 194512.

[29] D. Kane and R. Swason, "Measurement of the emitter saturation current by a contactless photoconductivity decay method," in *Proc. 18th IEEE Photovolt. Spec. Conf.*, vol. 18, 1985, pp. 578–583.

Authors' photographs and biographies not available at the time of publication.